

Femtosecond laser inscription of Bragg grating waveguides in bulk diamond

V. BHARADWAJ^{1,2,3}, A. COURVOISIER⁴, T. T. FERNANDEZ^{1,2}, R. RAMPONI^{1,2}, G. GALZERANO^{1,2}, J. NUNN⁵, M. J. BOOTH⁴, R. OSELLAME^{1,2}, S. M. EATON^{1,2,3}, P. S. SALTER^{4,*}

¹Istituto di Fotonica e Nanotecnologie-Consiglio Nazionale delle Ricerche (IFN-CNR), Piazza Leonardo da Vinci 32, Milano, Italy

²Department of Physics, Politecnico di Milano, Piazza Leonardo da Vinci 32, Milano, Italy

³Center for Nano Science and Technology, Istituto Italiano di Tecnologia, Milano, Italy

⁴Department of Engineering Science, University of Oxford, Parks Road, Oxford, UK

⁵Centre for Photonics and Photonic Materials, Department of Physics, University of Bath, North Road, Bath BA2 7AY, UK

*Corresponding author: patrick.salter@eng.ox.ac.uk

Femtosecond laser writing is applied to form Bragg grating waveguides in the diamond bulk. Type II waveguides are integrated with a single pulse point-by-point periodic laser modification positioned towards the edge of the waveguide core. These photonic devices, operating in the telecommunications band, allow for simultaneous optical waveguiding and narrowband reflection from a 4th order grating. This fabrication technology opens the way towards advanced 3D photonic networks in diamond for a range of applications.

Diamond has attracted great interest in the quantum optics community thanks to its nitrogen vacancy (NV) center, a naturally occurring impurity that is responsible for the pink coloration of diamond crystals. The NV spin state with the brighter luminescence yield can be exploited for spin readout, exhibiting millisecond spin coherence times at ambient temperature [1], comparable to trapped ions. In addition, the energy levels of the ground state triplet of the NV are sensitive to external fields. These properties make NVs attractive as a scalable platform for efficient nanoscale resolution sensing based on electron spins [2] and for quantum information systems [3]. In addition, the strong Raman coefficient of diamond is effective for Raman lasers [4]. These applications would benefit from a photonic platform, but due to diamond's hardness and chemical inertness, a mature fabrication toolkit has yet to be developed [5].

Recently, femtosecond laser writing demonstrated the formation of buried optical waveguides in single-crystal synthetic diamond [6, 7]. By laser inscribing two closely spaced modifications of reduced refractive index, 3D optical waveguides in bulk diamond were shown. Compared to reactive ion etching/photolithography [8, 9, 10] and ion irradiation [11] fabrication methods, femtosecond laser writing is advantageous due to its ability to pattern optical circuits out-of-plane with arbitrary 3D

designs in a single process step. Femtosecond laser writing can also produce high quality single NVs on-demand [12] and even coupled to pre-existing laser written optical circuits [13].

In addition to 3D optical waveguides, narrowband reflection elements which permit wavelength-selective filtering and feedback would be of great benefit for optical magnetometry, quantum information and Raman laser applications. By adopting the Bragg grating waveguide (BGW) femtosecond laser fabrication method developed for glasses [14, 15], we demonstrate the first BGW in bulk diamond, for simultaneous optical waveguiding and narrowband reflection.

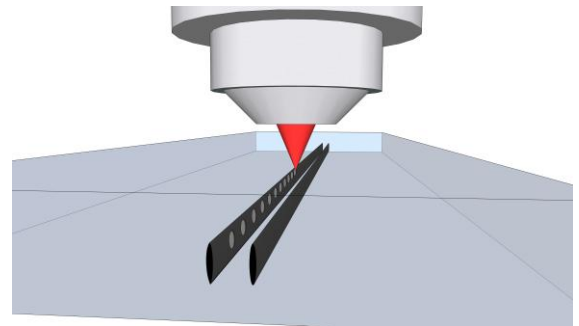


Fig. 1. Schematic Type II waveguide fabrication with embedded point-by-point grating shifted vertically upwards with respect to the waveguide.

Buried modifications were laser written in CVD single crystal diamond (Element 6) with dimensions of 3 mm × 3 mm × 0.5 mm using a Ti:Sapphire laser (wavelength 790 nm, pulse duration 250 fs, maximum repetition rate 1 kHz). A liquid crystal spatial light modulator (SLM) was employed to correct for spherical aberration introduced during focusing due to refraction at the diamond

interface [16]. The SLM was imaged onto the pupil plane of a high numerical aperture (NA) microscope objective (Olympus PlanApo 60 \times , 1.4 NA) using a 4*f* system. Correction of spherical aberration enabled the formation of submicron-dimension buried modifications at various depths within the diamond sample. Further details of the experimental setup can be found in Ref. [17]. To translate the sample with respect to the focused laser beam, three-axis air bearing translation stages (ABL1000, Aerotech) were employed.

Type II waveguides were formed with 1 kHz repetition rate, 80 nJ pulse energy and 0.1 mm/s scan speed. Using the adaptive optics described above to compensate for aberration, nearly symmetric tracks were formed, with transverse and vertical dimensions of 1 μm and 2 μm , respectively. The side walls of the type II waveguide were built up using 6 passes of the diamond through the laser focus, with a vertical translation of 3 μm per pass, leading to a final vertical dimension of 18 μm . For single mode waveguiding at the 1550-nm wavelength targeted in this study, a 25 μm separation between the side walls was employed.

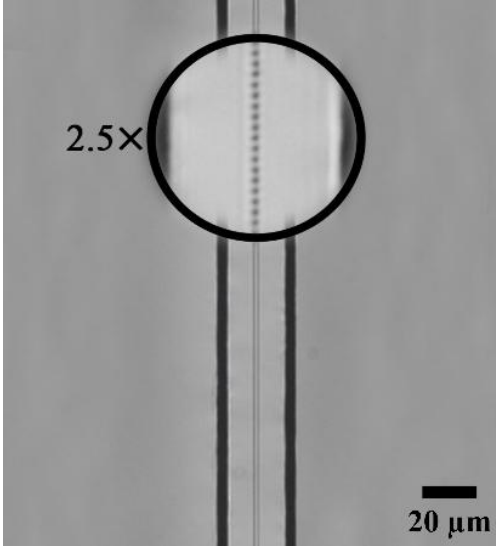


Fig. 2. Overhead optical microscope image of type II waveguide with a point-by-point periodic modulation in the center for Bragg reflection. Inset reveals a slightly refocused view with 2.5 \times increase in magnification, revealing the 1.3 μm pitch of the periodic modification within the type II waveguide.

After inscription of the side walls, a point-by-point periodic modulation was written all along the waveguide by lowering the repetition rate to $R = 100$ Hz and using a scan speed of $v = 0.13$ mm/s. This resulted in a grating pitch of $\Lambda = v/R = 1.3$ μm , as shown in Fig. 2. The periodic modulation was written with 1.5 μJ pulse energy, ~ 20 -fold higher than the pulse energy used to form the side walls. As such, the periodic element was significantly vertically elongated due to nonlinear propagation (Fig. 3). The center of the vertically extended side walls is 50 μm below the surface of diamond and the bottom edge of the transversely-centered periodic modulation extends 3 μm below the top edge of the side walls, as shown in Fig. 3. The periodic modulation was shifted upwards with respect to the waveguide mode to minimize propagation loss.

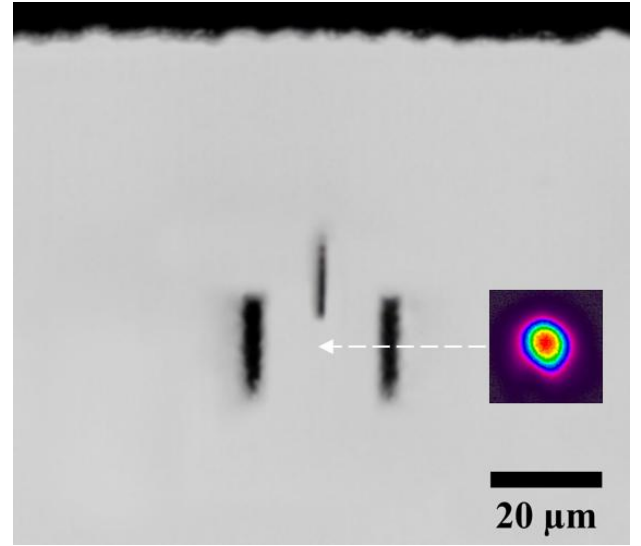


Fig. 3. Transverse optical microscope image of type II waveguide with side walls separated by 25 μm . The bottom edge of the transversely-centered point-by-point periodic modulation extends 3 μm below the top edge of the side walls. Inset shows the near field intensity of the guided mode at 1550-nm wavelength.

The resonant wavelength is given by the well-known Bragg condition [18]:

$$\lambda_B = 2n_{\text{eff}} \Lambda / m \quad (1)$$

where λ_B is the Bragg wavelength, n_{eff} is the effective modal index (DC refractive index) and m is the grating order. Estimating n_{eff} as the bulk refractive index (2.3878 at 1550 nm [19]), a Bragg reflection at 1550 nm wavelength for a 4th order grating is predicted.

Using a standard fiber-waveguide characterization setup [20] the mode field diameter (MFD) of the BGW was found to be 10 $\mu\text{m} \times 10$ μm (Fig. 3 inset) at 1560 nm wavelength, outside the Bragg reflection bandwidth. The single mode waveguides supported only the TM polarization. The out of band insertion loss of the BGW was 7.5 dB at 1560 nm, of which 3dB can be attributed to the presence of the point by point grating.

Using a broadband amplified spontaneous emission (ASE) source (ASE-100-C, IPG Laser GmbH) together with an optical spectrum analyzer (AQ6317C, Ando) with 10 pm resolution, the spectral transmission properties of the BGW were characterized. As shown in Fig. 4, a narrowband (FWHM = 290 pm) transmission dip was observed, centered at $\lambda_B = 1552.13$ nm. The strength of the dip was 6.3 dB, impressively high for a 4th order grating. The ~ 1 dB loss on the short wavelength side of the resonance is attributed to radiation mode losses.

The maximum reflectivity of a Bragg grating is given by [21]:

$$R_{\text{max}} = 1 - 10^{-\frac{T}{10}} = \tanh^2(\kappa L) \quad (2)$$

where T is the transmission dip in dB, κ is the coupling coefficient and L is the grating length (3 mm). Solving for the coupling coefficient, we obtain $\kappa = 450$ m⁻¹, yielding a grating strength $\kappa L = 1.4$, of similar strength as BGWs laser-written in other crystalline media [22, 23].

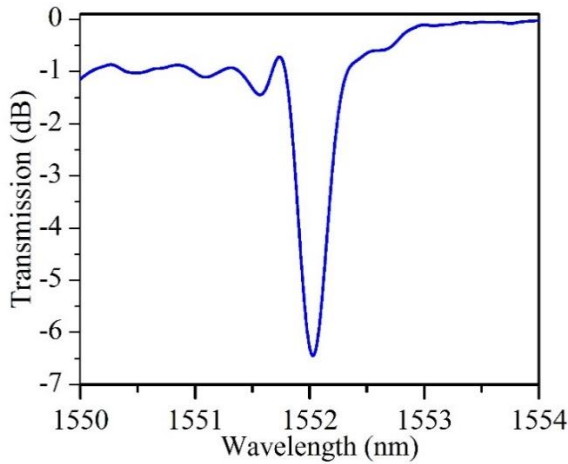


Fig. 4. Transmission spectrum of Bragg grating waveguide in diamond showing a 6.3 dB dip at $\lambda_B = 1552.13$ nm.

For glass-based BGWs, the reflection spectrum may be obtained using a known reflection from a fiber Bragg grating butt-coupled to the output facet of the waveguide [15]. However, for high refractive index diamond, Fresnel reflections at the diamond-glass fiber interface are present, which result in small Fabry-Perot fringes in the reflection spectrum observed out of band, as seen in Fig. 5. The reflectivity peak was calibrated using these Fabry-Perot cavity fringes [24]. The values given in the graph are in relative units of decibels giving a relative Bragg reflection peak of 5 dB with respect to the fringe background. From the full width at first zeroes bandwidth of the reflection spectrum [21]:

$$\Delta\lambda_{FWFZ} = \frac{\lambda^2}{\pi n_{\text{eff}} L} \sqrt{(\kappa L)^2 + \pi^2} = 367 \text{ pm} \quad (3)$$

we deduce a coupling coefficient of $\kappa = 460 \text{ m}^{-1}$, in excellent agreement with the transmission spectrum and Eq. (2).

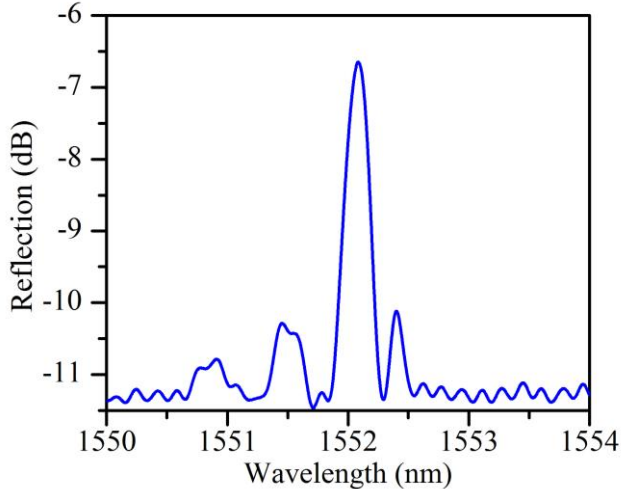


Fig. 5. Reflection spectrum of Bragg grating waveguide in diamond.

In summary, we have demonstrated laser written waveguides in the diamond bulk integrated with fourth order point by point Bragg gratings to give narrowband reflection in the telecommunications band. In future experiments, we will seek to form finer pitched modulations within the type II diamond waveguides, targeting shorter wavelength Bragg resonances for use in applications such

as Raman lasers [4] and magnetometry [25, 26]. Alternatively, taking advantage of diamond's ultrawide transparency window deep in the THz, larger pitched modulations will also be pursued to enable Bragg grating waveguides for a versatile range of sensing applications at mid to far infrared wavelengths [27].

Funding. SME is thankful for support from the DIAMANTE MIUR-SIR grant. PSS and MJB gratefully acknowledge the Leverhulme Trust (RPG-2013-044) and the UK Engineering and Physical Sciences Research Council (EP/K034480/1) for financial support.

Acknowledgements. We thank Dr. Haibin Zhang, Dr. J. P. Hadden and Prof. Michael Withford for enlightening scientific discussions.

References

1. G. Balasubramanian, P. Neumann, D. Twitchen, M. Markham, R. Kolesov, N. Mizuochi, J. Isoya, J. Achard, J. Beck, J. Tissler, V. Jacques, P. R. Hemmer, F. Jelezko, and J. Wrachtrup, *Nat. Mater.* 8, 383–387 (2009).
2. R. Schirhagl, K. Chang, M. Loretz, C. L. Degen, *Annual review of physical chemistry* 65, 83–105 (2014).
3. B. Hensen, H. Bernien, A. E. Dr  au, A. Reiserer, N. Kalb, M. S. Blok, J. Ruitenber, R. F. Vermeulen, R. N. Schouten, C. Abell  n, and W. Amaya, *Nature* 526, 682–686 (2015).
4. S. Reilly, V. G. Savitski, H. Liu, E. Gu, M. D. Dawson, and A. J. Kemp, *Opt. Lett.* 40, 930 (2015).
5. I. Aharonovich, A. D. Greentree, and S. Prawer, *Nature Photonics* 5, 397–405 (2011).
6. B. Sotillo, V. Bharadwaj, J. P. Hadden, M. Sakakura, A. Chiappini, T. T. Fernandez, S. Longhi O. Jedrkiewicz, Y. Shimotsuma, L. Criante, R. Osellame, G. Galzerano, M. Ferrari, K. Miura, R. Ramponi, P. E. Barclay, and S. M. Eaton, *Scientific Reports* 6, 35566 (2016).
7. A. Courvoisier, M. J. Booth, and P. S. Salter, *P. S., Appl. Phys. Lett.* 109, 031109 (2016).
8. M. P. Hiscocks, K. Ganesan, B. C. Gibson, S. T. Huntington, F. Ladouceur, and S. Prawer, *Opt. Express* 16, 19512–19519 (2008).
9. M. J. Burek, Y. Chu, M. S. Liddy, P. Patel, J. Rochman, S. Meesala, W. Hong, Q. Quan, M. D. Lukin, and M. Loncar, *Nat. Comm.* 5, 5718 (2014).
10. B. Khanaliloo, H. Jayakumar, A. C. Hryciw, D. P. Lake, H. Kaviani, and P. E. Barclay, *Phys. Rev. X* 5, 041051 (2015).
11. S. Lagomarsino, P. Olivero, F. Bosia, M. Vannoni, S. Calusi, L. Giuntini, and M. Massi, *Phys. Rev. Lett.* 105, 233903 (2010).
12. Y.-C. Chen, P. S. Salter, S. Knauer, L. Weng, A. C. Frangeskou, C. J. Stephen, S. N. Ishmael, P. R. Dolan, S. Johnson, B. L. Green, G. W. Morley, M. E. Newton, J. G. Rarity, M. J. Booth, and J. M. Smith, *Nature Photonics* 11, 77 (2016).
13. J. P. Hadden, V. Bharadwaj, S. Rampini, R. Osellame, J. Witmer, H. Jayakumar, T. T. Fernandez, A. Chiappini, C. Armellini, M. Ferrari, R. Ramponi, P. E. Barclay, S. M. Eaton, "Waveguide-coupled single NV in diamond enabled by femtosecond laser writing," *arXiv preprint arXiv:1701.05885* (2017).
14. G. D. Marshall, M. Ams, and M. J. Withford, *Opt. Lett.* 21, 2690 (2006).
15. H. Zhang, S. M. Eaton, and P. R. Herman, *Opt. Lett.* 32, 2559–2561 (2007).
16. R. D. Simmonds, P. S. Salter, A. Jesacher and M. J. Booth, *Opt. Express* 19, 24122–24128 (2011).
17. L. Huang, P. S. Salter, F. Payne, and M. Booth, *Opt. Express* 24, 10565 (2016).

18. W. L. Bragg, Proc. Cambr. Philos. Soci. 17, 43-57 (1914).
19. <https://refractiveindex.info/?shelf=3d&book=crystals&page=diamond>
20. B. Sotillo, V. Bharadwaj, J. P. Hadden, S. Rampini, A. Chiappini, T. T. Fernandez, C. Armellini, A. Serpengüzel, M. Ferrari, P. E. Barclay, Roberta Ramponi, and S. M. Eaton, Micromachines 8, 60 (2017).
21. T. Erdogan, IEEE Journal of Lightwave Technology 8, 1277-1294 (1997).
22. S. Kroesen, W. Horn, J. Imbrock, and C. Denz, Opt. Express 22, 23339-23348 (2014).
23. M. Ams, T. Calmano, B. F. Johnston, P. Dekker, C. Kränkel, and M. J. Withford, in *Photonics and Fiber Technology 2016 (ACOFT, BGPP, NP)*, OSA Technical Digest (online) (Optical Society of America, 2016), paper BM3B.3.
24. J. M. Vaughan, The Fabry-Perot interferometer (Adam Hilger, Bristol, 1989).
25. O. Gazzano, and C. Becher, Physical Review B 95, 115312 (2017).
26. H. Clevenson, M. E. Trusheim, C. Teale, T. Schröder, D. Braje, D. Englund, Nature Physics 11, 393–397 (2015).
27. M. Sieger and B. Mizaikoff, Analytical Chemistry, 88, 5562-5573 (2016).